The proton-activated ovarian cancer G protein-coupled receptor 1 (OGR1) is responsible for renal calcium loss during acidosis

Imenez Silva, Pedro Henrique ; Katamesh-Benabbas, Chahira ; Chan, Kessara ; Pastor Arroyo, Eva Maria ; Knöpfel, Thomas ; Bettoni, Carla ; Ludwig, Marie-Gabrielle ; Gasser, Jürg A ; Brandao-Burch, Andrea ; Arnett, Timothy R ; Bonny, Olivier ; Seuwen, Klaus ; Wagner, Carsten Alexander

Abstract: Hypercalciuria is a common feature during metabolic acidosis and associates to nephrolithiasis and nephrocalcinosis. The mechanisms sensing acidosis and inducing increased urinary calcium excretion are still unknown. Here we tested whether mice deficient for proton-activated Ovarian cancer G-protein coupled receptor 1 (OGR1 or Gpr68) have reduced urinary excretion of calcium during chronic metabolic acidosis. In the kidney, OGR1 mRNA was found in cells of the glomerulus, proximal tubule, and interstitium including endothelial cells. Wild type (OGR1+/+) and OGR1 knockout (OGR1−/−) mice were given standard chow without (control) or loaded with ammonium chloride for one or seven days to induce acute or chronic metabolic acidosis, respectively. No differences in responding to the acid load were observed in the knockout mice, except for higher plasma bicarbonate after one day. Bone mineral density, resorption activity of osteoclasts, and urinary deoxypyridinoline were similar between genotypes. During metabolic acidosis the expression levels of key proteins involved in calcium reabsorption, i.e. the sodium/proton exchanger (NHE3), the epithelial calcium-selective channel TRPV5, and the vitamin D-dependent calcium binding protein calbindin-D28k were all higher in the knockout mice compared to wild type mice. This is consistent with the previous demonstration that OGR1 reduces NHE3 activity and its surface expression in HEK293 cells. Wild-type mice displayed a non-linear positive association between urinary proton and calcium excretion which was lost in the knockout mice. Thus, OGR1 is a pH sensor involved in the hypercalciuria of metabolic acidosis by controlling NHE3 activity in the proximal tubule. Hence, novel drugs modulating OGR1 activity may improve renal calcium handling.

DOI: https://doi.org/10.1016/j.kint.2019.12.006

The proton-activated ovarian cancer G protein-coupled receptor 1 (OGR1) is responsible for renal calcium loss during acidosis

Pedro Henrique Imenez Silva[1,2,6], Chahira Katamesh-Benabbas[1,2,6], Kessara Chan[1,2], Eva Maria Pastor Arroyo[1,2], Thomas Knöpfel[1], Carla Bettoni[1,2], Marie-Gabrielle Ludwig[3], Jürg A. Gasser[3], Andrea Brandao-Burch[4], Timothy R. Arnett[4], Olivier Bonny[5], Klaus Seuwen[3] and Carsten Alexander Wagner[1,2]

[1]Institute of Physiology, University of Zurich, Zürich, Switzerland; [2]National Center for Competence in Research, NCCR Kidney.CH, Swiss National Science Foundation, Bern, Switzerland; [3]Novartis Institutes for Biomedical Research, Basel, Switzerland; [4]Department of Cell & Developmental Biology, University College London, London, UK; and [5]Department of Pharmacology and Toxicology, University of Lausanne, Lausanne, Switzerland

Hypercalciuria is a common feature during metabolic acidosis and associates to nephrolithiasis and nephrocalcinosis. The mechanisms sensing acidosis and inducing increased urinary calcium excretion are still unknown. Here we tested whether mice deficient for proton-activated Ovarian cancer G-protein coupled receptor 1 (OGR1 or *Gpr68*) have reduced urinary excretion of calcium during chronic metabolic acidosis. In the kidney, OGR1 mRNA was found in cells of the glomerulus, proximal tubule, and interstitium including endothelial cells. Wild type (OGR1$^{+/+}$) and OGR1 knockout (OGR1$^{-/-}$) mice were given standard chow without (control) or loaded with ammonium chloride for one or seven days to induce acute or chronic metabolic acidosis, respectively. No differences in responding to the acid load were observed in the knockout mice, except for higher plasma bicarbonate after one day. Bone mineral density, resorption activity of osteoclasts, and urinary deoxypyridinoline were similar between genotypes. During metabolic acidosis the expression levels of key proteins involved in calcium reabsorption, i.e. the sodium/proton exchanger (NHE3), the epithelial calcium-selective channel TRPV5, and the vitamin D-dependent calcium binding protein calbindin-D28k were all higher in the knockout mice compared to wild type mice. This is consistent with the previous demonstration that OGR1 reduces NHE3 activity and its surface expression in HEK293 cells. Wild-type mice displayed a non-linear positive association between urinary proton and calcium excretion which was lost in the knockout mice. Thus, OGR1 is a pH sensor involved in the hypercalciuria of metabolic acidosis by controlling NHE3 activity in the proximal tubule. Hence, novel drugs modulating OGR1 activity may improve renal calcium handling.

Kidney International (2020) ■, ■–■; https://doi.org/10.1016/j.kint.2019.12.006

KEYWORDS: acidosis; calcium; GPCR; hypercalciuria; NHE3; proton sensing

Translational Statement

Control of acid–base and mineral metabolism are major tasks of the kidney. The proton-activated receptor ovarian cancer G-protein coupled receptor 1 (OGR1 or *GPR68*) is expressed in many tissues including kidney. Its role in inflammatory and fibrosing disease makes the receptor an attractive pharmacological target while its role in kidney has remained elusive. Absence of OGR1 reduces renal calcium excretion during acidosis without other major effects on renal function. These data indicate that inhibitors of OGR1 may have few side effects on renal function and may even be useful in patients with elevated calcium excretion.

Acid–base status modulates renal handling of Ca^{2+} and Mg^{2+}. Both, metabolic and respiratory acidosis cause hypercalciuria.[1–7] Acidosis contributes to loss of Ca^{2+} from bones resulting in the development or worsening of bone disease.[8,9] The augmented intratubular concentration of calcium may promote nephrocalcinosis and nephrolithiasis.[10–12]

In kidney, Ca^{2+} and Mg^{2+} is mostly reabsorbed through passive paracellular routes in the proximal tubule and thick ascending limb of the loop of Henle (TAL) involving claudin 14 (CLDN14), CLDN16, and CLDN19 in the TAL. In the proximal tubule, transcellular Na^+ reabsorption involving the Na^+/H^+-exchanger isoform 3 (NHE3) drives paracellular water and Ca^{2+} absorption.[13] Active and regulated Ca^{2+} and Mg^{2+} reabsorption occurs in the distal convoluted tubule

Correspondence: *Carsten Alexander Wagner, Institute of Physiology and Zurich Center for Integrative Human Physiology, University of Zurich, Winterthurerstrasse 190, CH-8057 Zurich, Switzerland. E-mail: Wagnerca@access.uzh.ch*

[6]These authors contributed equally to this work and share first authorship.

Received 16 January 2019; revised 29 November 2019; accepted 5 December 2019; published online 25 December 2019

(DCT) and connecting tubule where the final amount of Ca^{2+} and Mg^{2+} excretion is determined by transcellular reabsorption through the apically localized epithelial transient receptor potential cation channel vanilloid 5 (TRPV5) Ca^{2+} channel and the transient receptor potential cation channel melastatin 6 (TRPM6) and TRPM7 Mg^{2+} channels.[14–16] Ca^{2+} and Mg^{2+} are reabsorbed in different proportions in each nephron segment and the expression pattern and regulation of TRPV5 and TRPM6 differ along the DCT and connecting tubule.[17] Reabsorbed Ca^{2+} is buffered intracellularly by calbindin-D28k and released across the basolateral membrane via Na^+/Ca^{2+}-exchanger 1 (NCX1) and plasma membrane Ca^{2+}–adenosine triphosphatases (ATPases) (PMCA).[18] TRPV5 channel expression and activity is regulated by various hormones and factors.[14,18] Among them, metabolic acidosis reduces TRPV5-mediated Ca^{2+} reabsorption, which may be due to a combination of direct inhibitory effects of protons on TRPV5 channel function and downregulation of channel expression, at least at mRNA level.[3,19–24] The molecular pH sensor that triggers renal hypercalciuria during acidosis has not been identified to date.

The proton-activated G-protein coupled receptors (GPRs) OGR1 (*Gpr68*), GPR4 (*Gpr4*), and T-cell death associated gene 8 (*Gpr65*) are inactive at pH around 7.8 and are maximally active at pH 6.8,[25,26] making them potential candidates to sense systemic and local pH within the physiologically relevant range. GPR4 is critical for the pH-regulated stimulation of ventilation and may participate in renal acid-sensing.[2,27] OGR1 has been implicated in the regulation of bone density and bone demineralization by low pH.[3–5,28,29] Mutations in OGR1/*GPR68* occur in patients with amelogenesis imperfecta.[30] OGR1 may also act as an endothelial flow sensor.[31]

OGR1 mRNA expression is widespread in most organs including bone and kidney.[32] In renal OGR1-transfected HEK293 cells, OGR1 modulates in a pH-dependent manner the activity of NHE3.[33]

Here we examined OGR1-deficient mice and found that OGR1 may play a major role in adapting renal calcium excretion during acidosis by regulating proteins involved in renal calcium transport.

RESULTS

Tissue distribution and segmental expression of OGR1 in mouse kidney

OGR1 mRNA was detected in all mouse organs tested with highest expression in spleen, testis, and lungs (Supplementary Figure S1). Qualitative OGR1 localization in kidney was further addressed by mRNA *in situ* hybridization (ISH). OGR1 mRNA was found in renal tubules, interstitial cells, glomeruli, and blood vessels, both in cortex and medulla (Figure 1). OGR1 mRNA was evidently more frequently observed in glomeruli, cells surrounding the glomerulus, and interstitial cells in the cortex, while tubular expression was less frequent (Figure 1a–f). No signal was detected in kidneys from $OGR1^{-/-}$ mice (Supplementary Figure S2). OGR1 mRNA levels were examined in nephron segments by quantitative polymerase chain reaction. It was detected in glomerulus and all nephron segments (Supplementary Figure S3) consistent with data retrieved from a single-cell RNA sequencing study in murine kidneys. OGR1 mRNA had been found in proximal tubules, loop of Henle, intercalated cells, fibroblasts, B and T lymphocytes, natural killer cells, and a novel cell type[34] (Figure 1h). In total kidney of $OGR1^{+/+}$ mice, OGR1 mRNA levels were not altered by metabolic acidosis during an acute (1-day) and more chronic (7-day) acid challenge (Figure 1g).

OGR1 does not play an essential role in systemic acid–base balance

Next, we tested whether OGR1 absence affects acid–base status with 1- and 7-day acid challenges. Under control conditions no differences in plasma [HCO_3^-], PCO_2, and pH between genotypes was detected (Supplementary Table S1). Urinary pH, phosphate, and NH_4^+ were similar in both groups (Supplementary Table S2). After 1-day acid-loading, $OGR1^{-/-}$ mice exhibited a milder metabolic acidosis with higher plasma [HCO_3^-] ($OGR1^{-/-}$: 18.3 ± 0.7 mmol/l vs. $OGR1^{+/+}$:13.7 ± 1.7 mmol/l), but only with a trend for higher plasma pH (median of $OGR1^{-/-}$: pH 7.17 vs. $OGR1^{+/+}$: pH 7.11, $P > 0.05$) (Supplementary Table S1). Abundance of proteins involved in renal acid–base handling were not different between $OGR1^{+/+}$ and $OGR1^{-/-}$ mice with an acute acid challenge, such as the ammoniagenic enzyme phosphate-dependent glutaminase, phosphoenolpyruvate carboxykinase, and the acid–base transporters sodium bicarbonate cotransporter 1, NHE3, and the B1 subunit of the H^+-ATPase (Supplementary Figure S4). No differences were observed after 7 days of acid-loading between $OGR1^{+/+}$ and $OGR1^{-/-}$ mice for plasma pH, [HCO_3^-], and PCO_2. Urinary pH and ammonium exhibited similar values between genotypes (Supplementary Table S3). Thus, we did not detect any evidence for a critical role of OGR1 in the renal control of acid–base balance. However, we did not further determine whether absence of OGR1 activity was compensated by other potential renal H^+ sensors.

OGR1 regulates renal Ca^{2+} handling during chronic metabolic acidosis

NH_4Cl-induced metabolic acidosis caused hypercalciuria in wild-type mice (Figure 2a). However, hypermagnesuria in wild-type mice was less evident (Figure 2b). In contrast, urinary Ca^{2+} (and Mg^{2+}) excretion did not increase in $OGR1^{-/-}$ mice (Figure 2a and b, Supplementary Table S2), whereas all other urinary electrolytes were similar between genotypes. Fractional excretion of Ca^{2+} and Mg^{2+} followed similar trends (Supplementary Figure S5A and B). Plasma calcium and magnesium concentrations were similar in all mice (Figure 2c and d; Supplementary Table S1). Total content of Ca^{2+} and Mg^{2+} in the stool corrected by the amount ingested were also not different between genotypes, but the total amount of calcium and magnesium absorbed by the intestine increased during 7 days of NH_4Cl-loading consistent

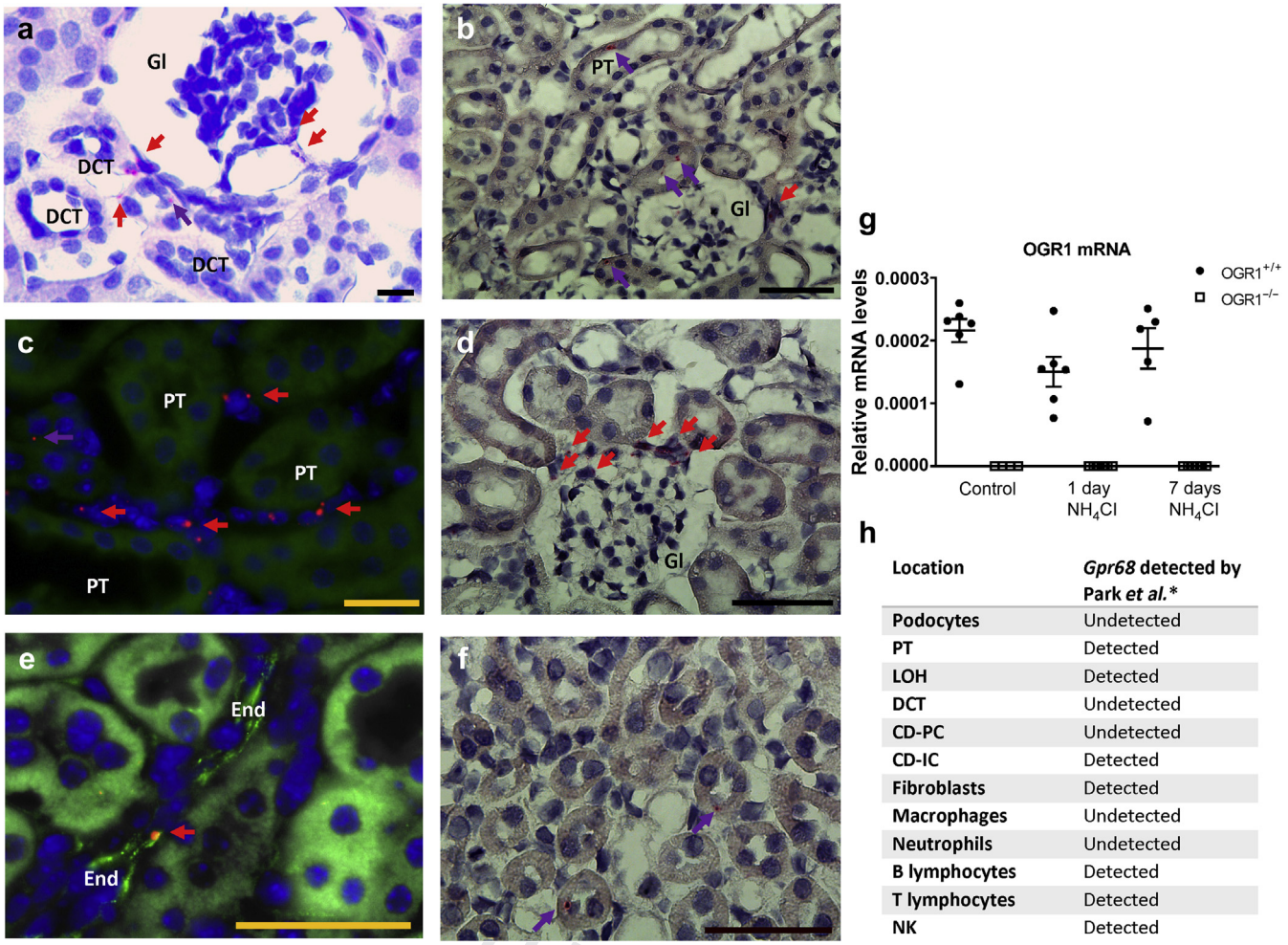

h

Location	*Gpr68* detected by Park *et al.**
Podocytes	Undetected
PT	Detected
LOH	Detected
DCT	Undetected
CD-PC	Undetected
CD-IC	Detected
Fibroblasts	Detected
Macrophages	Undetected
Neutrophils	Undetected
B lymphocytes	Detected
T lymphocytes	Detected
NK	Detected

Figure 1 | Expression of ovarian cancer G-protein coupled receptor 1 (OGR1) mRNA in kidney. (**a**) OGR1 mRNA was examined by *in situ* hybridization (ISH) in renal sections from OGR1$^{+/+}$ mice. Expression of OGR1 mRNA was observed by chromogenic ISH in interstitial cells and in tubules. OGR1 mRNA was often observed in periglomerular regions surrounded by distal convoluted tubules (DCTs). (**b**) Expression of OGR1 mRNA in proximal tubules. (**c**) Interstitial expression of OGR1 mRNA was also detected by fluorescent ISH. (**d**) Abundant expression of OGR1 mRNA in a glomerulus. (**e**) Colocalization of OGR1 mRNA with CD31, an endothelial marker, detected by immunofluorescence. (**f**) Tubular expression of OGR1 mRNA in the medulla. Red dots both in chromogenic and fluorescent ISH show OGR1 expression (red arrow). Chromogenic ISH sections were counterstained with hematoxylin I, showing nuclei in purple and fluorescent ISH sections were counterstained with 4′,6-diamidino-2-phenylindole, showing nuclei in blue. Rare tubular expression of OGR1 mRNA was indicated with purple arrows. (**g**) Expression of OGR1 mRNA was tested by quantitative polymerase chain reaction in RNA isolated from total kidney tissue from OGR1$^{+/+}$ and OGR1$^{-/-}$ mice during control conditions, 1 day or 7 days of NH_4Cl-loading. mRNA levels are given as $2^{-(Ct,\ OGR1\ -\ Ct,\ GAPDH)}$. Data are presented as mean ± SEM, $n = 5$ to 6 mice/group. (**h**) Positive or negative detection of OGR1 mRNA in different cell types by single-cell RNA sequencing, data retrieved from the study by Park *et al.*[34] Bars = 25 μm. CD, collecting duct, End, endothelial cells; Gl, glomerulus; IC, intercalated cells; LOH, loop of Henle; PC, principal cells; PT, proximal tubule; NK, natural killer cells. To optimize viewing of this image, please see the online version of this article at www.kidney-international.org.

with acidosis stimulated intestinal calcium absorption (Supplementary Figure S5C and D).[35–37] When urinary data from all dietary conditions were pooled, we observed a J-shaped curve describing the relationship between urinary [H^+] and calcium excretion in wild-type mice (quadratic polynomial, $R^2 = 0.55$) (Figure 3a). This relationship was absent in OGR1$^{-/-}$ mice (quadratic polynomial, $R^2 = 0.16$). Even more evident was the relationship between urinary [H^+] and NH_4^+, in which OGR1$^{-/-}$ mice showed a strong disruption in this relationship ($R^2 = 0.82$ vs. $R^2 = 0.18$) (Figure 3b). Creatinine clearance was reduced by chronic acid-loading in both genotypes (Figure 3c).

OGR1-dependent hypercalciuria is bone-independent

Increased bone resorption could increase urinary calcium excretion. To test whether the lack of increase of Ca^{2+} excretion into the urine is a consequence of lower osteoclastic activity in OGR1$^{-/-}$ mice, we isolated osteoclasts and stimulated cells *in vitro* by lowering medium pH. Similarly, osteoclast activity and its stimulation by extracellular pH were assessed by measuring resorbed areas on dentine discs (Figure 4a and b). Both male and female mice were examined separately. Low pH increased the area resorbed by osteoclasts[38,39] from both male and female wild-type mice (Figure 4a and b). Similar findings were obtained for

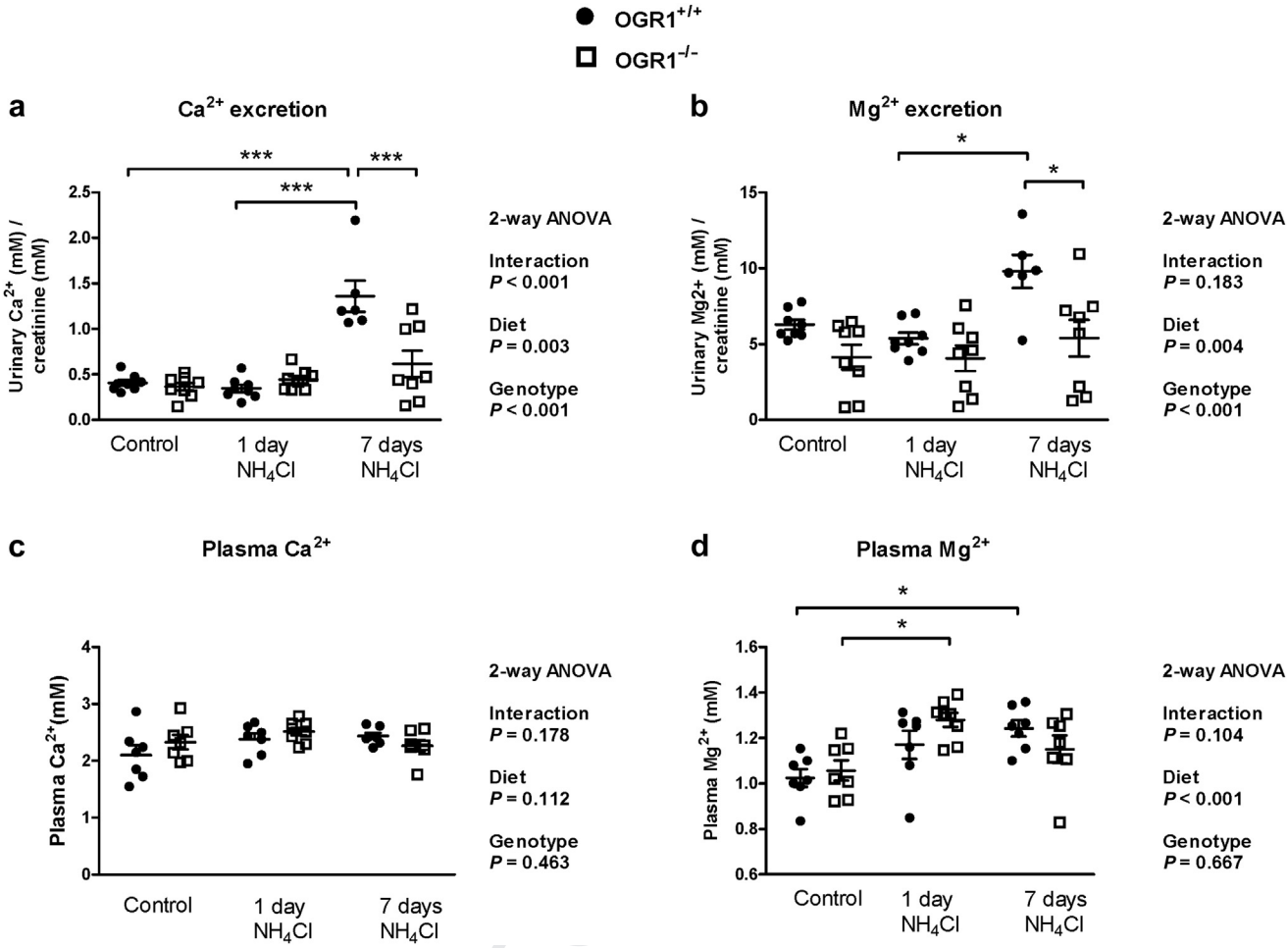

Figure 2 | Ovarian cancer G-protein coupled receptor 1 (OGR1)–deficient mice excrete less calcium in urine during chronic acid-loading. Urinary Ca^{2+} and Mg^{2+} excretion and plasma Ca^{2+} and Mg^{2+} concentrations were measured during metabolic acidosis in wild-type ($OGR1^{+/+}$) and OGR1 knockout mice ($OGR1^{-/-}$). Metabolic acidosis was induced by NH_4Cl-loading for 1 or 7 days. (**a**) Calcium excretion. (**b**) Magnesium excretion. (**c**) Plasma calcium and (**d**) magnesium levels were not affected by NH_4Cl-treatment and were comparable in wild-type and OGR1-deficient mice. Data are presented as mean ± SEM, $n = 6$ to 14 animals/group, $^*P < 0.05$, $^{***}P < 0.001$. ANOVA, analysis of variance; mM, mmol/l.

osteoclasts isolated from male and female $OGR1^{-/-}$ mice. No difference was observed between genotypes. To test for *in vivo* osteoclast activity, urinary deoxypyridinoline, a bone resorption marker, was measured in mice subjected to control and 7 days of NH_4Cl acid-loading. No difference was observed between genotypes, but a small effect of diet (i.e., control vs. NH_4Cl) was detected (Figure 4c). Next, we subjected male and female $OGR1^{+/+}$ and $OGR1^{-/-}$ mice to 8 weeks of acid-loading and control conditions. The proximal tibia metaphysis of 4-month-old skeletally mature mice were analyzed by peripheral quantitative computed tomography at baseline, as well as 4 and 8 weeks after induction of acidosis through the addition of 2% NH_4Cl to the drinking water. Total bone mineral density, cortical thickness, and cancellous bone mineral density showed no difference between $OGR1^{+/+}$ and $OGR1^{-/-}$ in both sexes (Figure 4d–i).

Normal levels of hormones

The plasma levels of parathyroid hormone (PTH) and $1,25(OH)_2$ vitamin D_3 were measured at baseline and after 7 days of NH_4Cl-loading. Seven days of acid-loading decreased levels of both hormones in the plasma, however, there was no difference between $OGR1^{+/+}$ and $OGR1^{-/-}$ mice (Supplementary Figure S6A and B).

Both acid-base balance and renal calcium handling are influenced by mechanisms involved in extracellular volume control, such as renal tubular fluid flow, delivery of salt and fluids to renal distal tubules, or aldosterone.[40–44] $OGR1^{+/+}$ and $OGR1^{-/-}$ mice had similar plasma and urinary Na^+ and K^+, body weight, urine volume, and plasma and urinary aldosterone levels (Supplementary Tables S1 and S2, and Supplementary Figure S6C and D), suggesting no major difference in extracellular volume status and control.

OGR1 regulates expression of renal proteins involved in Ca^{2+} reabsorption

To detect the expression of proteins apically expressed in the nephron, we used a preparation enriched for apical membranes. This enrichment protocol was validated using markers for various structures (Supplementary Figure S7). While

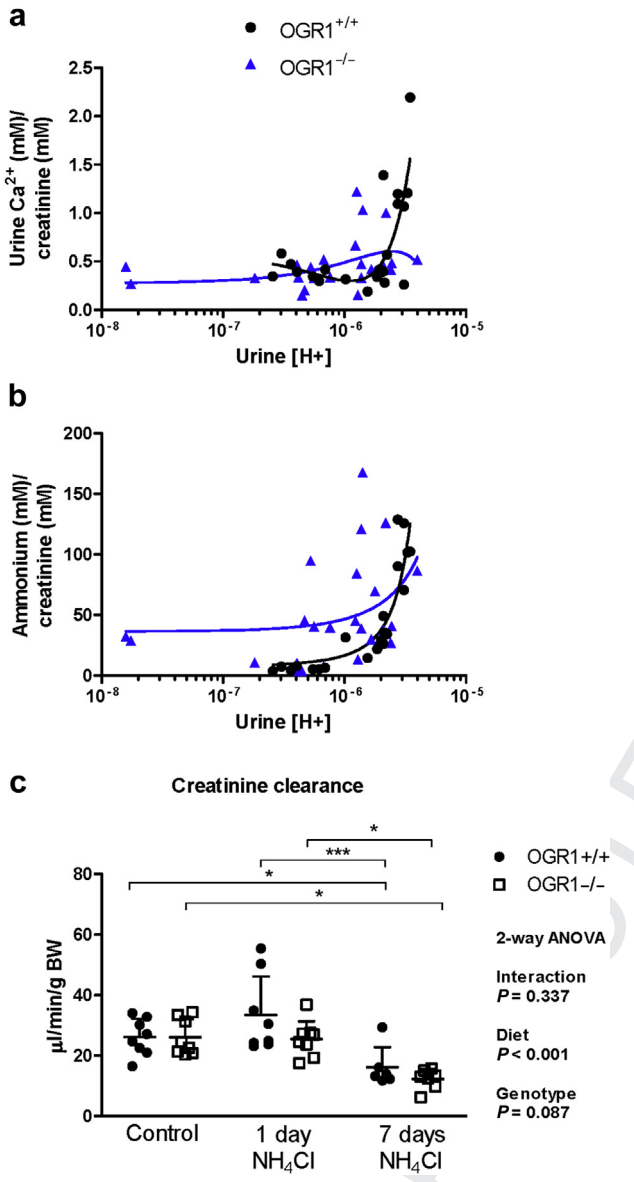

Figure 3 | Absence of ovarian cancer G-protein coupled receptor 1 (OGR1) alters the association between urinary [H^+] and calcium excretion, and urinary [H^+] and ammonium excretion without changes in creatinine clearance. (**a**) Second-order polynomial fitting for the relation between urinary [H^+] and Ca^{2+} excretion in $OGR1^{+/+}$ (black dots) and. $OGR1^{-/-}$ (blue triangles). (**b**) Second-order polynomial fitting for the relation between urinary [H^+] and NH_4^+ excretion in $OGR1^{+/+}$ (black dots) and. $OGR1^{-/-}$ (blue triangles). (**c**) Creatinine clearance in wild-type and OGR1-deficient mice. Data are presented as mean ± SEM, n = 6 to 8 animals/group, $^*P < 0.05$, $^{***}P < 0.001$. ANOVA, analysis of variance; BW, body weight; mM, mmol/l.

Golgi and endoplasmic reticulum markers were less abundant in apical membranes' preparation in comparison to total kidney lysates, lysosomal markers were enriched (Supplementary Figure S7).

We tested first the expression of NHE3, which is important for driving paracellular reabsorption of calcium in the proximal tubule. NHE3 abundance in a preparation enriched for apical membranes was not altered in $OGR1^{-/-}$ mice compared with wild-type mice under control conditions (Figure 5a), but NHE3 abundance was increased after 7 days of NH_4Cl-loading (118.5% increase in relative abundance in $OGR1^{-/-}$ vs. $OGR1^{+/+}$, $P = 0.027$) (Figure 5b). No difference was observed when NHE3 abundance was assessed in total kidney lysates after 7 days of NH_4Cl (Figure 5c). The ratio of NHE3 present in apical membranes versus total kidney lysate was also increased in $OGR1^{-/-}$ (Figure 5d). NHE3 is regulated by hormones and conditions such as PTH, angiotensin II, aldosterone, thyroid hormones, endothelin, glucocorticoids, acidosis, and others.[45] Plasma endothelin-1 levels were similar between $OGR1^{-/-}$ and $OGR1^{+/+}$, both under control and 7 days of NH_4Cl conditions (Supplementary Figure S8A). Endothelin-1 (*Edn1*) and endothelin receptor B (*Ednrb*) mRNA were not altered by diet or genotype (Supplementary Figure S8B and C). Renin is an essential enzyme for the production of angiotensin II. Renin mRNA levels were elevated in $OGR1^{-/-}$ mice, compared with $OGR1^{+/+}$ mice, after 7-day NH_4Cl load (Supplementary Figure S8D).

In the TAL, CLDN14, CLDN16, and CLDN19, required for the paracellular reabsorption of calcium and magnesium,[46] were not altered at mRNA level (Figure 5e–g). Immunoblotting for CLDN19 showed an expected band at ~20 kDa, which was not different between $OGR1^{+/+}$ and $OGR1^{-/-}$ (Figure 5h). We were not able to detect specific bands for CLDN16 with the antibodies available to us. Likewise, the abundance of the calcium-sensing receptor (CaSR), a regulator of TAL calcium reabsorption,[47–49] was not different between genotypes (Figure 5i).

Next, we assessed proteins participating in the active transepithelial transport of calcium in the late distal convoluted tubule and connecting tubule: TRPV5, calbindin-D28k, NCX1, and αklotho.[14,15,50] TRPV5 protein abundance in a preparation enriched with apical membranes showed no differences during control conditions between genotypes consistent with normal urinary calcium excretion (Figure 6a). In contrast, TRPV5 abundance was higher in apical membranes after 7 days of NH_4Cl-loading in $OGR1^{-/-}$ mice (91.5% higher densitometric value in $OGR1^{-/-}$ vs. $OGR1^{+/+}$, $P < 0.001$) (Figure 6b). The higher abundance of TRPV5 in $OGR1^{-/-}$ during NH_4Cl challenge suggests that TRPV5 is either upregulated in OGR1-deficient mice or downregulated by acidosis in the kidney of wild-type mice. Thus, we evaluated the effect of NH_4Cl-loading on TRPV5 abundance independently of genotype in $OGR1^{+/+}$ and $OGR1^{-/-}$. TRPV5 abundance was lowered in $OGR1^{+/+}$ subjected to NH_4Cl-loading, while no difference was observed in $OGR1^{-/-}$ (Figure 6c and d). Testing TRPV5 abundance in total kidney lysates of $OGR1^{+/+}$ and $OGR1^{-/-}$ mice during NH_4Cl-loading showed no difference between genotypes (Figure 6e). However, the ratio of TRPV5 in apical membranes versus total kidney lysate was not elevated in $OGR1^{-/-}$, suggesting that the redistribution of TRPV5 would be modest (Figure 6f). mRNA expression of the TRPV5 calcium channel was not different between genotypes and conditions

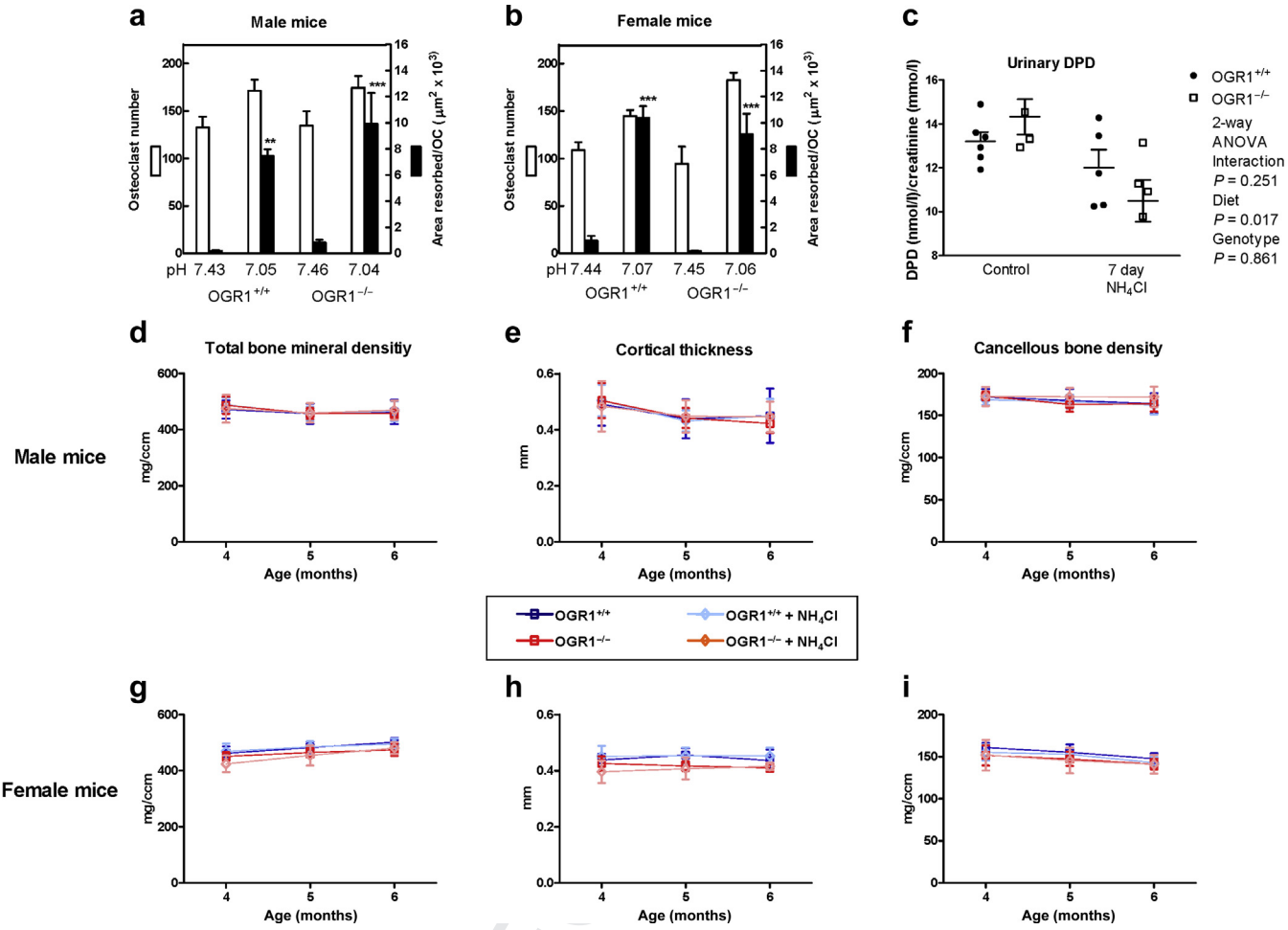

Figure 4 | No difference in osteoclast (OC) activity and bone parameters between ovarian cancer G-protein coupled receptor 1 (OGR1) wild-type and knockout mice. (**a,b**) Osteoclast number and bone resorbed area under control conditions (pH ~7.4) and acidosis (pH ~7.05) were determined *in vitro* after isolation of osteoclasts from (**a**) male and (**b**) female mice. (**c**) Urinary deoxypyridinoline (DPD), a marker of bone resorption in $OGR1^{+/+}$ and $OGR1^{-/-}$mice during control and 7 days of NH_4Cl-loading conditions. (**d–i**) Bone morphology data. (**d,g**) Total bone mineral density, (**e,h**) cortical thickness and (**f,i**) cancellous bone mineral density of $OGR1^{+/+}$ and $OGR1^{-/-}$ mice subjected to 8 weeks of acid-loading by NH_4Cl intake were determined on the proximal tibia metaphysis by peripheral quantitative computed tomography in (**d–f**) male and (**g–i**) female mice. No differences were detected for any parameter between genotypes. Data are presented as mean ± SEM for (**a,b**) 4 to 5 replicates, (**c**) 4 to 6 replicates, or (**d–i**) 10 replicates, $^{**}P < 0.01$, $^{***}P < 0.001$ comparing NH_4Cl treatment and control condition in the same genotype. ANOVA, analysis of variance.

(Figure 6g). However, a small increase in TRPV5 mRNA was observed in $OGR1^{-/-}$ at 7 days of NH_4Cl-loading when compared with control conditions.

Calbindin-D28k in total kidney lysates showed no differences during control conditions between genotypes (Figure 7a). However, calbindin-D28k protein levels were higher in $OGR1^{-/-}$ after 7-day NH_4Cl (+101.9% higher densitometric value in $OGR1^{-/-}$ vs. $OGR1^{+/+}$, $P = 0.002$) (Figure 7b). This elevation in calbindin-D28k was a result of a short trend of reduction in wild-type mice after 7-day NH_4Cl (−22% lower densitometric value in $OGR1^{-/-}$ vs. $OGR1^{+/+}$, $P = 0.115$) (Supplementary Figure S9A), and a larger increase in $OGR1^{-/-}$ due to acid-loading (+63.5% higher densitometric value in $OGR1^{-/-}$ vs. $OGR1^{+/+}$, $P = 0.035$) (Supplementary Figure S9B). The mRNA levels for calbindin-D28k were not different between genotypes (Supplementary Figure S9C). Because αklotho stabilizes TRPV5 at the luminal membrane,[51–54] we tested whether OGR1 regulates its protein levels in total kidney lysate. α-Klotho protein abundance was reduced in $OGR1^{-/-}$ mice (Figure 7c). Finally, we tested the protein levels of the basolateral Na^+/Ca^{2+} exchanger NCX1 mediating release of calcium into blood. NCX1 immunoblotting showed no difference in total kidney lysate preparations in metabolic acidosis between OGR1-deficient mice and wild-type mice (Figure 7d).

Because magnesium excretion had shown a trend to be decreased in NH_4Cl-loaded $OGR1^{-/-}$ mice, we tested the mRNA abundance of the TRPM6 and TRPM7 magnesium channels and found no difference (Supplementary Figure S10). Protein levels could not be examined due to the lack of specific antibodies.

FLA 5.6.0 DTD ■ KINT1893_proof ■ 5 February 2020 ■ 6:05 pm ■ ce

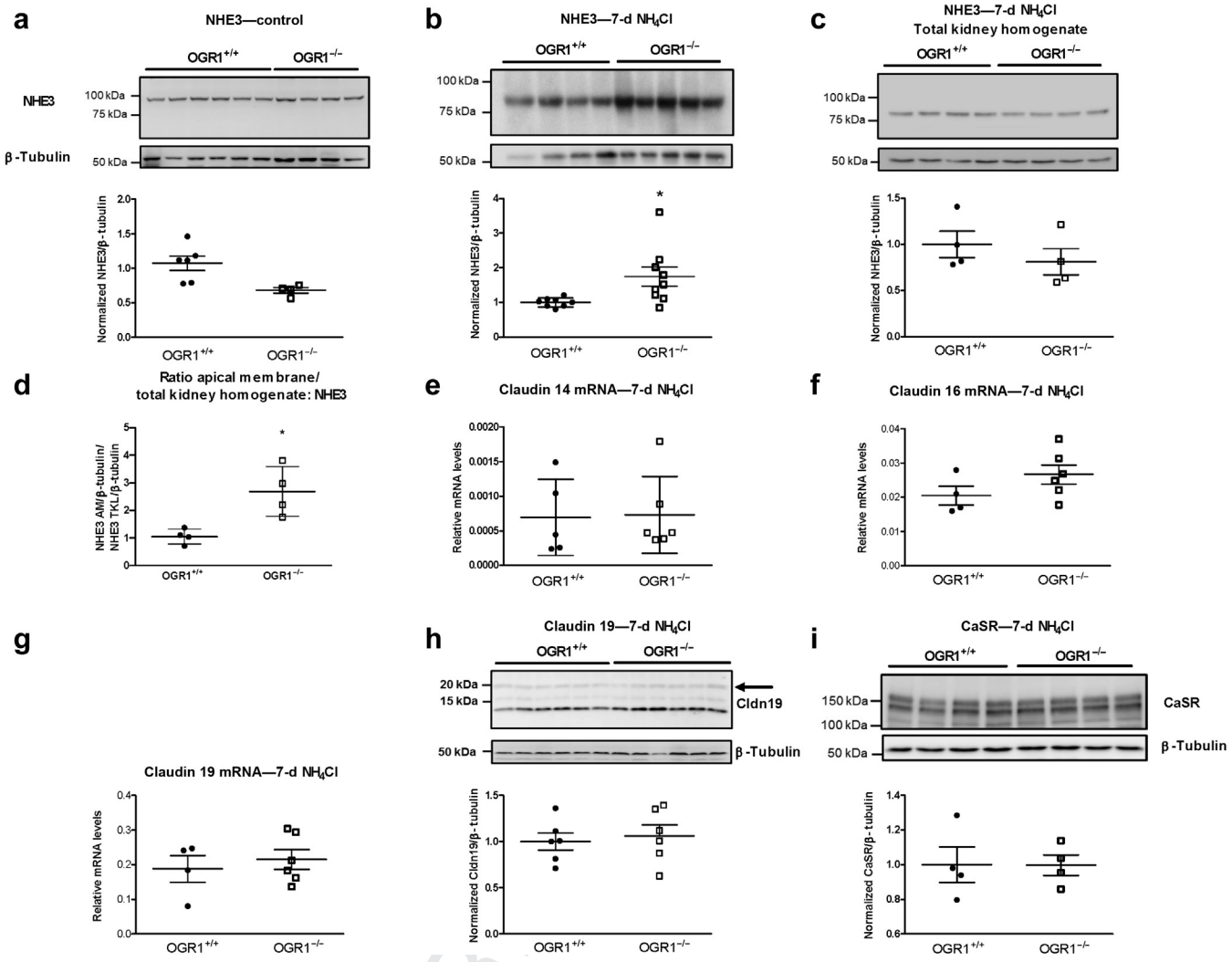

Figure 5| Ovarian cancer G-protein coupled receptor 1 (OGR1) modulates Na^+/H^+-exchanger isoform 3 (NHE3) expression but has no effect on proteins involved in reabsorption of calcium and magnesium in the thick ascending limb of the loop of Henle. The effects of OGR1 deletion and metabolic acidosis was tested on the expression of key molecules involved in calcium and magnesium reabsorption in the proximal tubule and the thick ascending limb of the loop of Henle. (**a**) Immunoblotting for NHE3 protein in renal apical membranes' preparations during control conditions. (**b**) NHE3 protein after 7 days of acid-loading. (**c**) Immunoblotting for NHE3 in total kidney lysate preparation (TKL). (**d**) Ratio of apical membrane (AM) to total kidney lysate densitometric values for NHE3. Renal mRNA expression of (**e**) claudin (Cldn) 14, (**f**) claudin 16, and (**g**) claudin 19. (**h**) Protein abundance of claudin 19 was assessed by immunoblotting. (**i**) Calcium-sensing receptor (CaSR) protein expression was evaluated by immunoblotting in renal total kidney lysates of mice subjected to 7 days of acid-loading. Scatter plots represent densitometric values normalized to (**a,b,d,e**) β-tubulin or (**c**) mRNA levels given as $2^{(Ct,\ OGR1\ -\ Ct,\ HPRT)}$. Data are presented as mean ± SEM, $n = 4$ to 9 mice per group, $^*P < 0.05$. To optimize viewing of this image, please see the online version of this article at www.kidney-international.org.

DISCUSSION

Hypercalciuria occurs frequently during acidosis.[5,55,56] Hypercalciuria occurs even under restricted calcium intake, suggesting a renal Ca^{2+} leak.[7] Experiments in various rodent models suggest that metabolic or respiratory acidosis stimulate intestinal calcium absorption.[35–37] Thus, renal losses of calcium are probably set off by increased intestinal Ca^{2+} absorption, thereby maintaining extracellular Ca^{2+} balance. Here we demonstrate that mice deficient for OGR1 lack the typical calcium hyperexcretion during chronic acid-loading and we show that OGR1 negatively regulates NHE3 membrane expression. Moreover, TRPV5 and calbindin-D28k are increased in OGR1-deficient mice under chronic metabolic acidosis.

Renal calcium excretion depends on the filtered load and tubular transport mechanisms. We first tested for extrarenal causes of hypercalciuria. We did not detect differences in fecal calcium and magnesium content indicative of similar intestinal absorption rates for both cations. However, fecal content of calcium was slightly reduced by chronic acidosis in both genotypes, reflecting increased intestinal calcium absorption.[36,57] OGR1 is expressed in bone.[25,29,58–63] However, controversial data on a bone phenotype exist, reporting no abnormalities in 1 model and increased bone density in

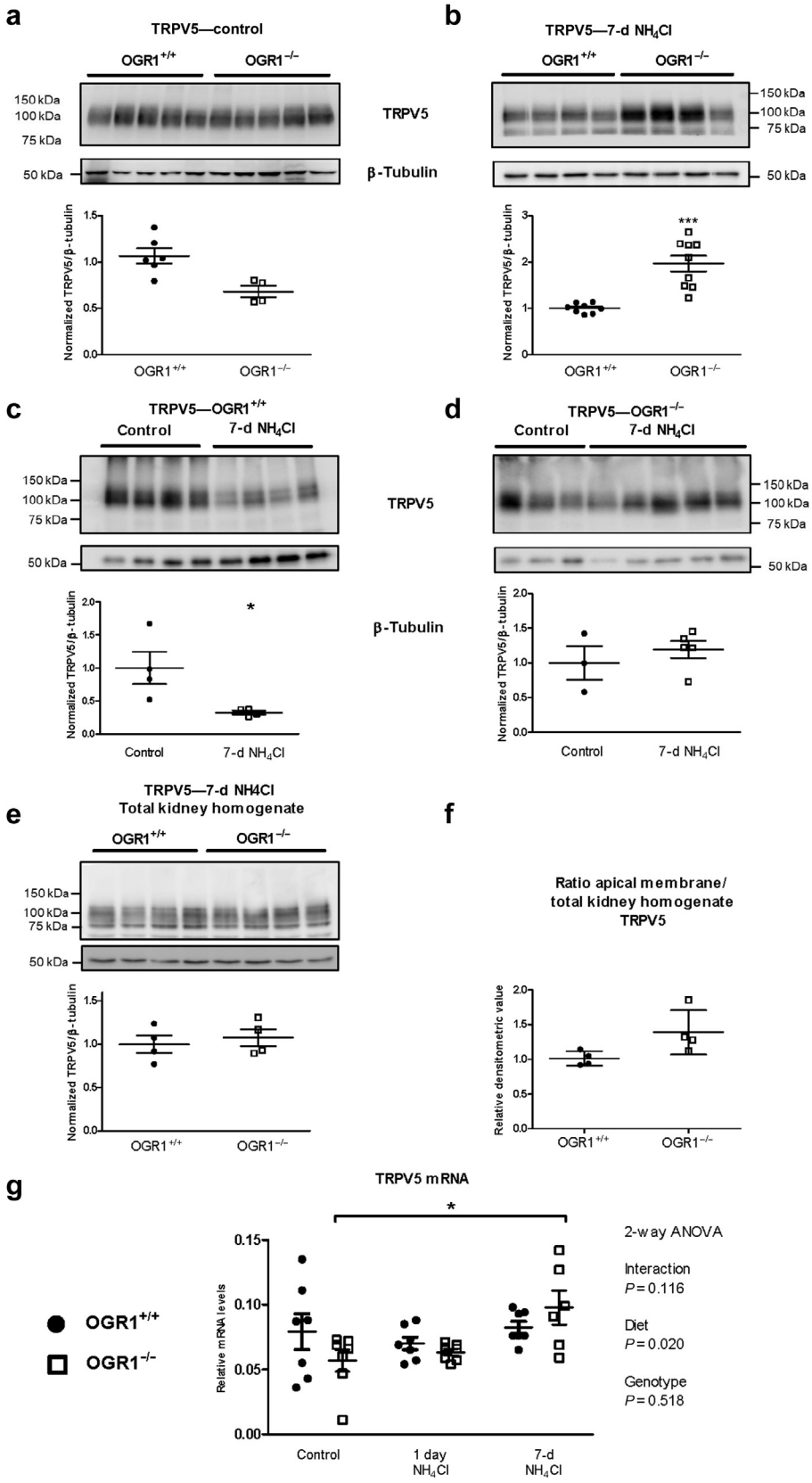

Figure 6 | Ovarian cancer G-protein coupled receptor 1 (OGR1) regulates the transient receptor potential cation channel vanilloid 5 (TRPV5) calcium channel during acidosis. (**a–d**) TRPV5 protein abundance in renal apical membrane preparations. Comparison between (**a,b**) genotypes or (**c,d**) acid–base conditions were examined by immunoblotting. (**a**) TRPV5 abundance in OGR1$^{+/+}$ and OGR1$^{-/-}$ mice under control condition. (**b**) OGR1$^{+/+}$ and OGR1$^{-/-}$ mice after 7 days of acid-loading. (**c**) OGR1$^{+/+}$ under control condition and (continued)

very young mice lacking OGR1.[60,63] Krieger *et al.*[60] demonstrated a mild trabecular/cortical bone phenotype in skeletally immature, rapidly growing male mice. Their bone phenotype determined at age 8 weeks captures the potential role of OGR1 during fast skeletal growth (postnatal to puberty), whereas we initiated our challenge at skeletal maturity at 4 months of age, when skeletal growth is no longer active. Some of the effects that Krieger *et al.*[60] demonstrated, such as the effect on cortical osteoblasts (periosteal formation drifts) and on micromodeling drifts in the secondary spongiosa (their region of interest), can no longer occur in our adult mice, because the cortical and cancellous formation drifts are no longer active. Additionally, osteoclastic bone resorption is well-known to be activated by acidosis,[38,39] but we did not find any evidence for a critical pH-sensing role of OGR1 in osteoclast function *in vitro* or for bone density *in vivo,* suggesting that the function of OGR1 in bone is not primarily responsible for hypercalciuria in wild-type mice. Plasma levels of both divalent cations, excretion of all urine electrolytes, diuresis, creatinine clearance, and aldosterone levels (indicating similar volume status and regulation) were similar in both genotypes, suggesting that the total filtered load and overall tubular function was not different between genotypes.

The role of OGR1 in kidney may be critical for the hypercalciuria during chronic acid-loading. Renal calcium reabsorption is mediated by distinct mechanisms located in the proximal tubule, the TAL, and the late DCT and connecting tubule. We examined changes in key molecules involved in calcium reabsorption in these segments.

Proximal tubular calcium reabsorption occurs mostly via the paracellular route driven by the lumen positive potential and paracellular fluid fluxes due to active transcellular solute and sodium transport. NHE3 contributes largely to active sodium absorption, and deletion of NHE3 reduces calcium reabsorption.[13] In $OGR1^{-/-}$ mice, when compared with $OGR1^{+/+}$ mice, NHE3 abundance was higher during chronic, but not during acute acid-loading. We cannot exclude that NHE3 activity is regulated in the acute setting independent of protein abundance. Consistently, we had previously found that lowering pH in isolated proximal tubules from OGR1-deficient mice within minutes stimulated NHE3 activity more so than in tubules from wild-type animals.[33] Thus, enhanced proximal tubular NHE3 activity in the absence of OGR1 may contribute to decreased urinary calcium excretion in acid-loaded $OGR1^{-/-}$ mice. The same mechanism may also be responsible for the higher plasma bicarbonate levels in $OGR1^{-/-}$ after 1 day of NH_4Cl challenge.

Reabsorption of calcium in the TAL is via paracellular route involving CLDN14, CLDN16, and CLDN19.[64,65] We did not find any difference in the expression of Cldn16 and Cldn19. Moreover, the paracellular permeability of the TAL to calcium and magnesium is regulated by the calcium-sensing receptor[49] and interactions between OGR1 and the CaSR occur in brain,[66] but CaSR abundance was similar between genotypes. Therefore, our results did not provide evidence that the TAL is involved in the calcium-saving effect of OGR1 deletion.

The final tuning of urinary calcium excretion is achieved by regulated and active transcellular reabsorption in the late DCT and connecting segment. It involves the apically located TRPV5 calcium channel, the intracellular calcium buffer calbindin-D28k, and the basolateral Ca^{2+}-ATPase PMCA (the contributions of PMCA1 and PMCA4 isoforms to calcium reabsorption in the DCT or connecting tubule or both are still debated[67]) and sodium-calcium exchanger NCX1.[14,15,18] Calcium reabsorption by these proteins is stimulated by PTH and $1,25(OH)_2$ vitamin D_3, but levels of both hormones were similar in both genotypes and were reduced during chronic acid-loading. However, expression of TRPV5 protein was higher in a preparation enriched with apical membranes in $OGR1^{-/-}$ mice after 7 days of NH_4Cl challenge, whereas TRPV5 abundance was unchanged at baseline. The higher expression of TRPV5 in $OGR1^{-/-}$ mice under metabolic acidosis could be due to increase of TRPV5 expression in $OGR1^{-/-}$ and/or a decrease of TRPV5 abundance in $OGR1^{+/+}$ by metabolic acidosis. Further analyses revealed that apical TRPV5 is decreased in wild-type mice subjected to acid-loading consistent with a previous study reporting lower immunostaining intensity in kidneys from acidotic animals.[3] Total TRPV5 protein abundance in acidotic mice was similar between genotypes. This result can be interpreted in at least 2 distinct manners: (i) The lack of OGR1, by stimulating NHE3 activity, increases calcium reabsorption in the proximal tubule, which in turn causes a compensatory response in the distal tubule to increase reabsorption of calcium. This situation is reminiscent of the effect of thiazide diuretics on renal calcium handling where it is thought that salt and volume depletion leads to a compensatory increase in proximal salt reabsorption via NHE3 driving proximal paracellular Ca^{2+} reabsorption. The effect on distal calcium transport proteins is controversial and may include a compensatory increase in TRPV5 and calbindin-D28k expression.[68–71] (ii) OGR1 induces an internalization of TRPV5 channels in wild-type animals when acidotic. Both scenarios might be correct; however, we and others were not able to detect OGR1

Figure 6 | (continued) after 7 days of acid-loading. (**d**) $OGR1^{-/-}$ mice under control condition and after 7 days of acid-loading. (**e**) Immunoblotting for TRPV5 in total kidney lysate preparation. (**f**) Ratio of apical membrane to total kidney lysate densitometric values for TRPV5. (**g**) Renal mRNA expression levels of the epithelial Ca^{2+} channel TRPV5 were assessed by quantitative polymerase chain reaction in mice under control conditions or after 1 or 7 days of acid-loading. Membranes were stripped and reprobed for β-tubulin. (**a–d**) Scatter plots summarize densitometric data normalized to β-tubulin. Data are presented as mean ± SEM, $n = 3$ to 9 mice/group. *$P < 0.05$, **$P < 0.05$, ***$P < 0.001$. To optimize viewing of this image, please see the online version of this article at www.kidney-international.org.

FLA 5.6.0 DTD ■ KINT1893_proof ■ 5 February 2020 ■ 6:05 pm ■ ce

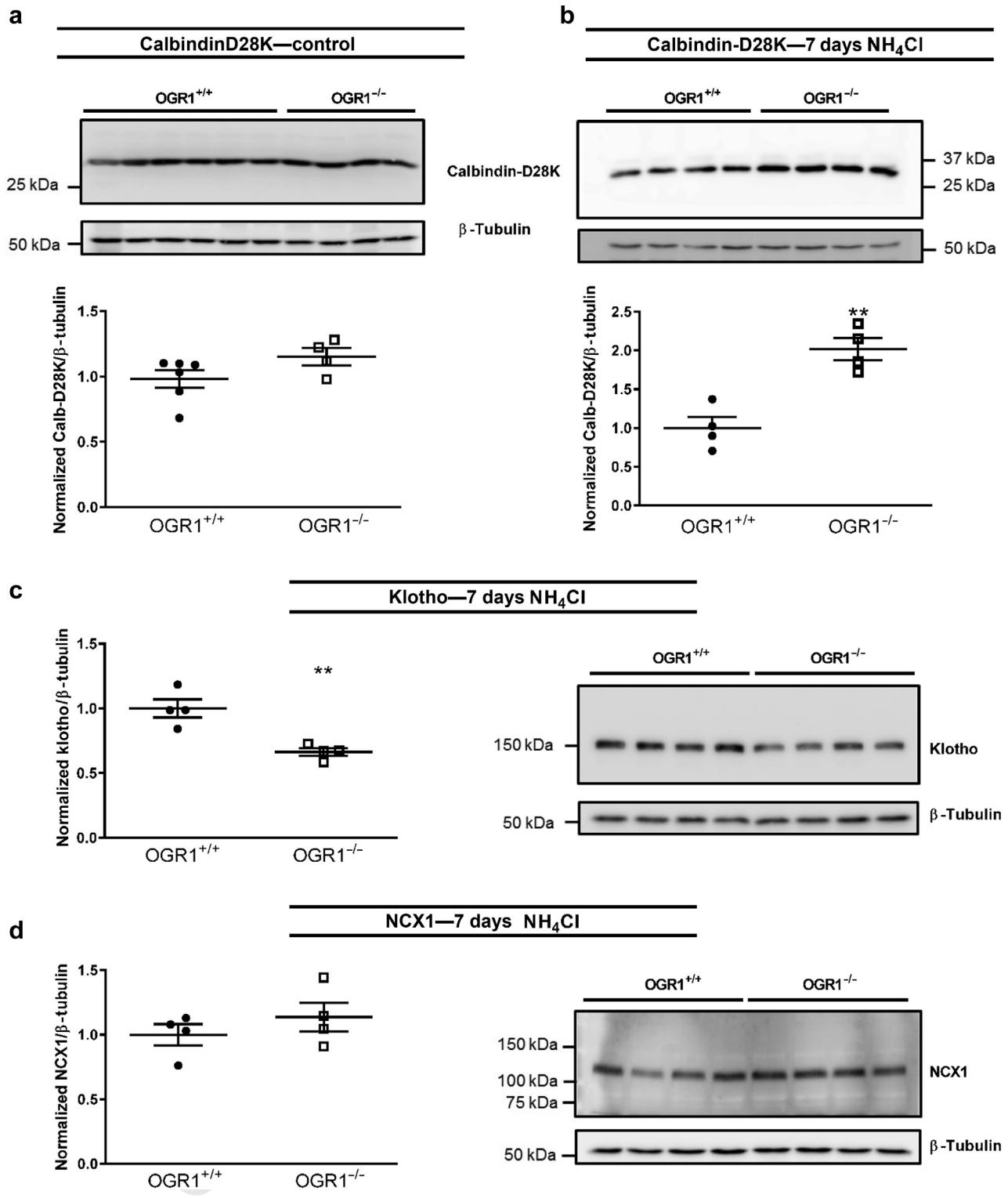

Figure 7 | Expression of proteins involved in distal convoluted calcium reabsorption in ovarian cancer G-protein coupled receptor 1 (OGR1)$^{+/+}$ and OGR1$^{-/-}$ mice. (**a**) Calbindin (Calb)-D28k abundance in mice during control conditions. (**b**) Calbindin-D28k abundance in mice after 7 days of acid-loading, and (**c**) α-klotho abundance in mice after 7 days of acid-loading. (**d**) Na^+/Ca^{2+} exchanger isoform 1 (NCX1) in mice after 7 days of acid-loading. Membranes were stripped and reprobed for β-tubulin. Scatter plots summarize densitometric data normalized to β-tubulin. Data are presented as mean ± SEM, $n = 4$ to 6 mice/group. $^{**}P < 0.01$. To optimize viewing of this image, please see the online version of this article at www.kidney-international.org.

expression in the DCT,[34] suggesting that the interaction between OGR1 and TRPV5, if it occurs, would be indirect. Nevertheless, in both cases, TRPV5 is a key player in acidosis-induced hypercalciuria as mice lacking *Trpv5* show no further increment in urinary calcium excretion during acidosis.[3] Also, mathematical modeling predicted reduced TRPV5-mediated calcium absorption during acidosis.[72] Acidosis may reduce TRPV5 activity through several mechanisms, by direct interactions of protons with the channel or indirectly by regulating pathways modulating TRPV5 activity and/or membrane abundance.[19–24] Direct inhibition of TRPV5 channels by extracellular protons is most pronounced when pH is lowered from pH 8 to pH 6;[22,24] however, this mechanism may play only a minor role in the acidosis-associated hypercalciuria. Measurements of urinary acidification as well as modeling of luminal pH demonstrates that urine pH is in the range of pH 6.8 to pH 6.1 in the late DCT and connecting tubule under normal conditions and during acidosis.[73] Thus, acid-loading would not increase TRPV5 inhibition due to luminal proton concentrations. Moreover, hypercalciuria in wild-type animals developed with a delay of >1 day and was not observed in the group acid-loaded for 24 hours despite nearly maximal urinary acidification. Similarly, intracellular protons inhibit TRPV5 channel activity, but intracellular pH is most likely more acidic during acute acid-loading before renal and extrarenal compensatory mechanisms are fully activated.[23] Data describing the regulation of renal calbindin-D28k by acid–base challenges are scarce. Both elevation and reduction in calbindin-D28k expression were observed in animals subjected to chronic NH_4Cl challenges.[3,4] Our data demonstrate that both the entry pathway into the DCT cells for calcium (i.e., TRPV5) and the intracellular buffer calbindin-D28k are coregulated by chronic acidification in an OGR1-dependent fashion. However, our apical membranes' preparation also enriches for lysosomal proteins; therefore, we cannot exclude that the increase in TRPV5 levels in OGR1 knockout mice reflects at least partially an increase in lysosomal TRPV5.

Thus, our data suggest that stimulation of OGR1 during acidosis constitutes a braking system, avoiding exaggerated calcium reabsorption in the proximal tubule. In parallel, acidosis causes a redistribution of TRPV5 channels from the membrane into an intracellular compartment along with reduction of calbindin-D28k. Both mechanisms grant the kidneys the ability to generate hypercalciuria in response to acidosis. However, when the OGR1-NHE3 axis is defective, kidney loses the capacity to properly coordinate urine acidification and calcium excretion. Other calcium-independent effects also occur, as ammonium excretion is also dysregulated in OGR1-deficient mice.

OGR1 activation increases intracellular inositol-1,4,5-trisphosphate and calcium but may also be linked to changes in cyclic adenosine monophosphate and extracellular signal–regulated kinase 1/2.[25,28,33,58,74] Inositol-1,4,5-trisphosphate, intracellular calcium, and extracellular signal–regulated kinase 1/2 all regulate NHE3 activity in kidneys and other organs.[75–78] In OGR1-transfected HEK293 cells, OGR1 activation increased intracellular calcium and suppressed NHE3 activity in a protein kinase C–dependent manner.[33]

Using ISH, OGR1 mRNA was found at low levels in renal epithelial cells but was frequently found in extratubular structures, most likely representing immune cells, fibroblasts, smooth muscle cells, and endothelial cells. A recent report demonstrated expression of OGR1 in endothelial cells and smooth muscle cells in colon.[79] These findings might suggest that OGR1- and pH-dependent signals may originate from renal blood vessels or interstitial cells and could further contribute to the modulation of tubular transport processes. Our previous demonstration that absence of OGR1 altered the pH response of isolated proximal tubules demonstrates that, at least in this segment, OGR1 is functionally expressed and regulates transport processes.[33]

Our study provides the first evidence that OGR1 plays an essential role in detecting low pH in the kidney and is critical for inducing the acidosis-associated hypercalciuria. OGR1 may provide a novel target to treat hypercalciuria with or without acidosis and the effect of recently developed specific OGR1 inhibitors and agonists remains to be tested.[80,81] OGR1 agonists may stimulate renal Ca^{2+} losses and should be monitored for long-term effects on Ca^{2+} balance.

METHODS

For detailed methods, please see Supplementary Methods.

Animal studies

Experiments were performed on $OGR1^{-/-}$ and $OGR1^{+/+}$ male mice of 12 to 14 weeks of age, 25 to 30 g. Generation and use of these mice has been described previously.[33]

All experiments were performed according to Swiss Animal Welfare laws and approved by the local veterinary authority (Veterinäramt Zürich).

Measurements of PTH, calcitriol, aldosterone, endothelin-1, and deoxypyridinoline

Hormones were measured using specific enzyme-linked immunosorbent assay and radioimmunoassay kits.

Osteoclast formation and activity measurements

Osteoclast formation and activity were investigated using cultures derived from the bone marrow of both male and female $OGR1^{-/-}$ and $OGR1^{+/+}$ mice, using methods similar those previously described.[34]

Statistical analysis

Statistical analyses were performed using GraphPad Prism 6 (Version 6.07; GraphPad Software Inc., San Diego, CA). Results are shown as mean ± SEM, except for pH values, which are represented as median and first and third quartiles. Data were tested using unpaired Student *t*-test or 2-way analysis of variance followed by Tukey multiple comparison test as appropriate. Comparisons of $[H^+]$ concentrations were tested with Kruskal-Wallis.

For the *in vivo* assessment of bone morphology experiments, statistical analyses were carried out using RS/Client 2.1.2. for Windows (Build Number 4.32, RS/1 Version 6.0.1, 1999; Domain

Manufacturing Corp., Burlington, MA) or SAS software (SAS Institute, Cary, NC). Data were subjected to 1-way analysis of variance. Equality of variances was tested by the Levene F test. Multiple-group comparisons were analyzed using the Dunnett test. For all the tests $\alpha = 0.05$.

DISCLOSURE

All the authors declared no competing interests.

ACKNOWLEDGMENTS

This study was supported by grants from the Swiss National Science Foundation (31003A_155959) and the Novartis Foundation for Medical and Biological Research to CAW. PHIS received a fellowship from the IKPP Kidney.CH under the European Union's Seventh Framework Programme for Research, Technological Development, and Demonstration under the grant agreement 608847 and Conselho Nacional de Desenvolvimento Científico e Tecnológico grant 205625/2014-2. CB received a ZIHP PhD student fellowship. The use of the ZIRP Core facility for Rodent Physiology is gratefully acknowledged. We thank Norman P. Curthoys, Nina Himmerkus, Markus Bleich, Jianghui Hou, and Johannes Loffing for providing antibodies. We thank Joana Delgado Martins and Milica Bugarski for helping with the identification of different nephron segments in immunohistochemistry images. Lastly, we thank Nima Yassini and David Pentón Ribas for technical support.

AUTHOR CONTRIBUTIONS

PHIS, CK-B, KC, EMPA, TK, CB, M-GL, and AB-B performed experiments. PHIS, CK-B, M-GL, JAG, OB, KS, and CAW designed the experiments. PHIS, CKB, KC, EMPA, TK, CB, M-GL, JG, AB-B, TRA, OB, KS, and CAW reviewed the manuscript and edited the manuscript. PHIS, CK-B, and CAW wrote the manuscript. All authors read and approved the manuscript.

SUPPLEMENTARY MATERIAL

Supplementary File (PDF)

Supplementary Methods.

Figure S1. OGR1 mRNA was detected in all tested organs. mRNA levels are given as $2^{-(Ct,\ OGR1\ -\ Ct,\ GAPDH)}$ normalized to kidney. Data are presented as means ± SEM, $n = 3$.

Figure S2. In situ hybridization (ISH) specifically detected OGR1 mRNA. (**A,B**) OGR1 mRNA was not detected in renal tissue from OGR1$^{-/-}$ mice. (**C**) Assay and tissue quality were tested with the positive control peptidyl-prolyl cis-trans isomerase B in OGR1$^{+/+}$ and (**D**) OGR1$^{-/-}$ mice (***Ppib***). Bars = 28.5 µm.

Figure S3. OGR1 mRNA expression was examined in murine hand-dissected glomeruli and nephron segments. mRNA levels are given as $2^{-(Ct,\ OGR1\ -\ Ct,\ GAPDH)}$ normalized to glomeruli. Data are presented as mean ± SEM, $n = 3$ to 6 glomeruli/segment.

Figure S4. OGR1 does not affect the expression of proteins involved in the renal control of acid–base balance in response to acute metabolic acidosis. (**A**) Immunoblotting for NHE3. (**B**) NBCe1. (**C**) B1 subunit of H^+-ATPase. (**D**) PEPCK. (**E**) Phosphate-dependent glutaminase (PDG/GLS) with its 2 forms: KGA (65 kDa) and GAC (60 kDa). Western blotting was performed using total kidney lysates, except for (**A**) NHE3, which was performed using a preparation enriched for apical membranes. Membranes were stripped and reprobed for β-tubulin as loading control. Scatter plots represent densitometric analyses of protein abundance normalized to β-tubulin. Data are presented as mean ± SEM, $n = 5$ to 6 mice/group.

Figure S5. Urinary fractional excretion of calcium, magnesium, and phosphate, as well as fecal excretion of calcium and magnesium in OGR1$^{+/+}$ and OGR1$^{-/-}$ mice under control conditions and after 1 or 7 days of acid-loading. Fractional excretion of (**A**) calcium, (**B**) magnesium, and (**C**) phosphate. (**D**) Total fecal calcium excretion over 24 hours. (**E**) Total fecal magnesium excretion over 24 hours. Fecal excretion was normalized to the respective divalent cation intake. (**F**) Second-order polynomial curves fitting the correlation between urine $[H^+]$ and fraction of excretion of Ca^{2+} for OGR1$^{+/+}$ ($R^2 = 0.47$, $n = 20$) and OGR1$^{-/-}$ ($R^2 = 0.07$, $n = 22$). (**A–E**) Data are presented as mean ± SEM, $n = 6$ to 8 mice/group. $^*P < 0.05$, $^{**}P < 0.01$.

Figure S6. Acid-loading but not absence of OGR1 affected parathyroid hormone, 1,25-$(OH)_2$ vitamin D_3 levels, and aldosterone. (**A**) Plasma PTH and (**B**) plasma 1,25$(OH)_2$ vitamin D_3 levels were decreased during metabolic acidosis in OGR1$^{+/+}$ and OGR1$^{-/-}$ mice subjected to 7 days of acid-loading. (**C**) Urinary and (**D**) plasma aldosterone levels were equally affected by 7 days of acid-loading in OGR1$^{+/+}$ and OGR1$^{-/-}$. Data are presented as mean ± SEM, $n = 4$ to 7 mice per group. $^*P < 0.05$, $^{**}P < 0.01$, $^{***}P < 0.001$.

Figure S7. Apical membranes' enrichment protocol enriches for renal epithelial apical membranes and lysosomal membranes. Red arrows show the expected band size. β-Tubulin immunoblot is shown as a reference below each immunoblot image. Ap.M., apical membranes; DCT, distal convoluted tubule; ER, endoplasmic reticulum; LAMP1, lysosomal associated membrane protein 1; NaPi-IIa (*Slc34a1*), sodium phosphate cotransporter 2A; NCC (*Slc12a3*), sodium chloride cotransporter; NPC1, Niemann-Pick disease type C1; PT, proximal tubule; Tot. H., total kidney homogenate.

Figure S8. Expression levels of regulators of NHE3 activity and abundance. (**A**) Endothelin-1 plasma levels. (**B**) Endothelin-1 (*Edn1*) mRNA levels. (**C**) Endothelin receptor B, ETB (*Ednrb*) mRNA levels. (**D**) Renin (*Ren*) mRNA levels. Renal mRNA expression levels were assessed by qPCR in mice under control conditions or after 1 or 7 days of acid-loading. Data are presented as mean ± SEM, $n = 3$ to 6 mice/group. $^{**}P < 0.01$.

Figure S9. Effects of 7 days of NH_4Cl-loading on calbindin-D28k abundance. (**A**) Calbindin-D28k abundance in OGR1$^{+/+}$ mice. (**B**) Calbindin-D28k abundance in OGR1$^{-/-}$ mice. (**C**) Renal mRNA expression levels of the intracellular calcium buffer calbindin-D28k were assessed by qPCR in mice under control conditions or after 1 or 7 days of acid-loading. Membranes were stripped and reprobed for β-tubulin. Densitometric values were normalized for β-tubulin values and then normalized to control values. Data are presented as mean ± SEM, $n = 4$ to 6 mice/group. $^*P < 0.05$.

Figure S10. Ablation of OGR1 has no effect on mRNA abundance of TRPM6 and TRPM7 magnesium channels. (**A**) mRNA abundance of the magnesium channels TRPM6 and (**B**) TRPM7 were assessed in kidney by qPCR. mRNA levels are given as $2^{-(Ct,\ OGR1\ -\ Ct,\ HPRT)}$. Data are presented as mean ± SEM, $n = 5$ to 7 mice/group. $^*P < 0.05$.

Table S1. Summary of blood analyses. Blood was collected from mice kept under control conditions, after 1 or 7 days of NH_4Cl-loading. Mice were anesthetized with isoflurane. Data are presented as means ± SEM. *Significantly different between *Ogr1*$^{+/+}$ and *Ogr1*$^{-/-}$ for the same treatment; $^*P \le 0.05$, $^{**}P \le 0.01$, $^{***}P \le 0.001$. $^{\#}$Significantly different between control group and treated group for the same genotype; $^{\#}P \le 0.05$, $^{\#\#}P \le 0.01$, $^{\#\#\#}P \le 0.001$. $^{\&}$Significantly different between treated groups 1 day versus 7 days of NH_4Cl for the same genotype; $^{\&}P \le 0.05$, $^{\&\&}P \le 0.01$, $^{\&\&\&}P \le 0.001$.

Table S2. Summary of urine analyses. Urine was collected in metabolic cages from mice kept under control conditions, after 1 or 7 days of NH_4Cl-loading. Data are presented as mean ± SEM. *Significantly different between *Ogr1*$^{+/+}$ and *Ogr1*$^{-/-}$ for the same treatment; $^*P \le 0.05$, $^{**}P \le 0.01$, $^{***}P \le 0.001$. $^{\#}$Significantly different between control group and treated group for the same genotype; $^{\#}P \le 0.05$, $^{\#\#}P \le 0.01$, $^{\#\#\#}P \le 0.001$. $^{\&}$Significantly different between

treated groups 1 day versus 7 days of NH_4Cl for the same genotype; $^{\&}P \leq 0.05$, $^{\&\&}P \leq 0.01$, $^{\&\&\&}P \leq 0.001$.

Table S3. Sequences of primers and probes used for semi-quantitative RT real-time PCR.

REFERENCES

1. Dai L-J, Ritchie G, Kerstan D, et al. Magnesium transport in the renal distal convoluted tubule. *Physiol Rev*. 2001;81:51–84.
2. Hoenderop JGJ, Nilius B, Bindels RJM. Calcium absorption across epithelia. *Physiol Rev*. 2005;85:373–422.
3. Nijenhuis T, Renkema KY, Hoenderop JGJ, et al. Acid-base status determines the renal expression of Ca2+ and Mg2+ transport proteins. *J Am Soc Nephrol*. 2006;17:617–626.
4. Rizzo M, Capasso G, Bleich M, et al. Effect of chronic metabolic acidosis on calbindin expression along the rat distal tubule. *J Am Soc Nephrol*. 2000;11:203–210.
5. Stacy BD, Wilson BW. Acidosis and hypercalciuria: renal mechanisms affecting calcium, magnesium and sodium excretion in the sheep. *J Physiol*. 1970;210:549–564.
6. Stehle RL, McCarty AC. The effect of hydrochloric acid ingestion upon the composition of the urine in man. *J Biol Chem*. 1921;47:315–319.
7. Farquharson RF, Salter WT, Tibbetts DM, et al. Studies of calcium and phosphorus metabolism. *J Clin Invest*. 1931;10:221–249.
8. Bushinsky DA. Net calcium efflux from live bone during chronic metabolic, but not respiratory, acidosis. *Am J Physiol Renal Physiol*. 1989;256:F836–F842.
9. Kraut JA, Kurtz I. Metabolic acidosis of CKD: diagnosis, clinical characteristics, and treatment. *Am J Kidney Dis*. 2005;45:978–993.
10. Evan AP. Physiopathology and etiology of stone formation in the kidney and the urinary tract. *Pediatr Nephrol*. 2009;25:831–841.
11. Khan SR. Nephrocalcinosis in animal models with and without stones. *Urol Res*. 2010;38:429–438.
12. Renkema KY, Velic A, Dijkman HB, et al. The calcium-sensing receptor promotes urinary acidification to prevent nephrolithiasis. *J Am Soc Nephrol*. 2009;20:1705–1713.
13. Pan W, Borovac J, Spicer Z, et al. The epithelial sodium/proton exchanger, NHE3, is necessary for renal and intestinal calcium (re) absorption. *Am J Physiol Renal Physiol*. 2012;302:F943–F956.
14. Dimke H, Hoenderop JGJ, Bindels RJM. Molecular basis of epithelial Ca2+ and Mg2+ transport: insights from the TRP channel family. *J Physiol*. 2011;589:1535–1542.
15. Boros S, Bindels RJM, Hoenderop JGJ. Active Ca2+ reabsorption in the connecting tubule. *Pflügers Arch*. 2009;458:99–109.
16. van der Wijst J, Bindels RJM, Hoenderop JGJ. Mg2+ homeostasis: the balancing act of TRPM6. *Curr Opin Nephrol Hypertens*. 2014;23:361–369.
17. Hsu Y-J, Hoenderop JGJ, Bindels RJM. TRP channels in kidney disease. *Biochim Biophys Acta*. 2007;1772:928–936.
18. Graaf SFJ van de, Bindels RJM, Hoenderop JGJ. Physiology of epithelial Ca2+ and Mg2+ transport. In: Amara SG, ed. *Reviews of Physiology, Biochemistry and Pharmacology*. Berlin, Germany: Springer; 2007:77–160.
19. Bonny O, Rubin A, Huang C-L, et al. Mechanism of urinary calcium regulation by urinary magnesium and pH. *J Am Soc Nephrol*. 2008;19:1530–1537.
20. Bindels RJ, Hartog A, Abrahamse SL, et al. Effects of pH on apical calcium entry and active calcium transport in rabbit cortical collecting system. *Am J Physiol Renal Physiol*. 1994;266:F620–F627.
21. Vennekens R, Prenen J, Hoenderop JG, et al. Modulation of the epithelial Ca2+ channel ECaC by extracellular pH. *Pflügers Arch*. 2001;442:237–242.
22. Yeh B-I, Kim YK, Jabbar W, et al. Conformational changes of pore helix coupled to gating of TRPV5 by protons. *EMBO J*. 2005;24:3224–3234.
23. Cha S-K, Jabbar W, Xie J, et al. Regulation of TRPV5 single-channel activity by intracellular pH. *J Membr Biol*. 2007;220:79–85.
24. Yeh B-I, Sun T-J, Lee JZ, et al. Mechanism and molecular determinant for regulation of rabbit transient receptor potential type 5 (TRPV5) channel by extracellular pH. *J Biol Chem*. 2003;278:51044–51052.
25. Ludwig M-G, Vanek M, Guerini D, et al. Proton-sensing G-protein-coupled receptors. *Nature*. 2003;425:93–98.
26. Wang J-Q, Kon J, Mogi C, et al. TDAG8 Is a proton-sensing and psychosine-sensitive G-protein-coupled receptor. *J Biol Chem*. 2004;279:45626–45633.
27. Kumar NN, Velic A, Soliz J, et al. Regulation of breathing by CO_2 requires the proton-activated receptor GPR4 in retrotrapezoid nucleus neurons. *Science*. 2015;348:1255–1260.
28. Pereverzev A, Komarova SV, Korčok J, et al. Extracellular acidification enhances osteoclast survival through an NFAT-independent, protein kinase C-dependent pathway. *Bone*. 2008;42:150–161.
29. Komarova SV, Pereverzev A, Shum JW, et al. Convergent signaling by acidosis and receptor activator of NF-κB ligand (RANKL) on the calcium/calcineurin/NFAT pathway in osteoclasts. *Proc Natl Acad Sci U S A*. 2005;102:2643–2648.
30. Parry DA, Smith CEL, El-Sayed W, et al. Mutations in the pH-sensing G-protein-coupled receptor GPR68 cause amelogenesis imperfecta. *Am J Hum Genet*. 2016;99:984–990.
31. Xu J, Mathur J, Vessières E, et al. GPR68 senses flow and is essential for vascular physiology. *Cell*. 2018;173:762–775.e16.
32. Xu Y, Casey G. Identification of human OGR1, a novel G protein-coupled receptor that maps to chromosome 14. *Genomics*. 1996;35:397–402.
33. Mohebbi N, Benabbas C, Vidal S, et al. The proton-activated G protein coupled receptor OGR1 acutely regulates the activity of epithelial proton transport proteins. *Cell Physiol Biochem*. 2012;29:313–324.
34. Park J, Shrestha R, Qiu C, et al. Single-cell transcriptomics of the mouse kidney reveals potential cellular targets of kidney disease. *Science*. 2018;360:758–763.
35. Cao JJ, Nielsen FH. Acid diet (high-meat protein) effects on calcium metabolism and bone health. *Curr Opin Clin Nutr Metab Care*. 2010;13:698–702.
36. Charoenphandhu N, Tudpor K, Pulsook N, Krishnamra N. Chronic metabolic acidosis stimulated transcellular and solvent drag-induced calcium transport in the duodenum of female rats. *Am J Physiol Gastrointest Liver Physiol*. 2006;291:G446–G455.
37. Canzanello VJ, Kraut JA, Holick MF, et al. Effect of chronic respiratory acidosis on calcium metabolism in the rat. *J Lab Clin Med*. 1995;126:81–87.
38. Orriss IR, Arnett TR. Rodent osteoclast cultures. In: Helfrich MH, Ralston SH, eds. *bone research protocols*. 816. Totowa, NJ: Humana Press; 2012:103–117.
39. Arnett T, Dempster D. Effect of pH on bone resorption by rat osteoclasts in vitro. *Endocrinology*. 1986;119:119–124.
40. Wilcox CS, Granges F, Kirk G, et al. Effects of saline infusion on titratable acid generation and ammonia secretion. *Am J Physiol Renal Physiol*. 1984;247:F506–F519.
41. Massry S, Coburn J, Chapman L, et al. Effect of NaCl infusion on urinary Ca++ and Mg++ during reduction in their filtered loads. *Am J Physiol*. 1967;213:1218–1224.
42. Leclerc M, Brunette MG, Couchourel D. Aldosterone enhances renal calcium reabsorption by two types of channels. *Kidney Int*. 2004;66:242–250.
43. Wagner CA. Effect of mineralocorticoids on acid-base balance. *Nephron Physiol*. 2014;128:26–34.
44. Lee C-T, Chen H-C, Lai L-W, et al. Effects of furosemide on renal calcium handling. *Am J Physiol Renal Physiol*. 2007;293:F1231–F1237.
45. Kurtz I. Molecular mechanisms and regulation of urinary acidification. In: Terjung R, ed. *Comprehensive Physiology*. Hoboken, NJ: John Wiley & Sons, Inc.; 2014:1737–1774.
46. Gong Y, Renigunta V, Himmerkus N, et al. Claudin-14 regulates renal Ca ++ transport in response to CaSR signalling via a novel microRNA pathway: claudin-14 function and regulation. *EMBO J*. 2012;31:1999–2012.
47. Ikari A, Okude C, Sawada H, et al. Activation of a polyvalent cation-sensing receptor decreases magnesium transport via claudin-16. *Biochim Biophys Acta*. 2008;1778:283–290.
48. Yu ASL. Claudins and the kidney. *J Am Soc Nephrol*. 2015;26:11–19.
49. Toka HR, Pollak MR, Houillier P. Calcium sensing in the renal tubule. *Physiology*. 2015;30:317–326.
50. Loffing J, Loffing-Cueni D, Valderrabano V, et al. Distribution of transcellular calcium and sodium transport pathways along mouse distal nephron. *Am J Physiol Renal Physiol*. 2001;281:F1021–F1027.
51. Chang Q, Hoefs S, Kemp AW van der, et al. The ß-glucuronidase klotho hydrolyzes and activates the TRPV5 channel. *Science*. 2005;310:490–493.
52. Cha S-K, Ortega B, Kurosu H, et al. Removal of sialic acid involving klotho causes cell-surface retention of TRPV5 channel via binding to galectin-1. *Proc Natl Acad Sci U S A*. 2008;105:9805–9810.

53. Alexander RT, Woudenberg-Vrenken TE, Buurman J, et al. Klotho prevents renal calcium loss. *J Am Soc Nephrol*. 2009;20:2371–2379.
54. Wolf MTF, An S-W, Nie M, et al. Klotho up-regulates renal calcium channel transient receptor potential vanilloid 5 (TRPV5) by intra- and extracellular N-glycosylation-dependent mechanisms. *J Biol Chem*. 2014;289:35849–35857.
55. Alexander RT, Cordat E, Chambrey R, et al. Acidosis and urinary calcium excretion: insights from genetic disorders. *J Am Soc Nephrol*. 2016;27:3511–3520.
56. Sayer JA. Progress in understanding the genetics of calcium-containing nephrolithiasis. *J Am Soc Nephrol*. 2017;28:748–759.
57. Gafter U, Edelstein S, Hirsh J, et al. Metabolic acidosis enhances 1,25(OH)2D3-induced intestinal absorption of calcium and phosphorus in rats. *Miner Electrolyte Metab*. 1986;12:213–217.
58. Saxena H, Deshpande D, Tiegs B, et al. The GPCR OGR1 (GPR68) mediates diverse signalling and contraction of airway smooth muscle in response to small reductions in extracellular pH. *Br J Pharmacol*. 2012;166:981–990.
59. Frick KK, Krieger NS, Nehrke K, Bushinsky DA. Metabolic acidosis increases intracellular calcium in bone cells through activation of the proton receptor OGR1. *J Bone Miner Res*. 2009;24:305–313.
60. Krieger NS, Yao Z, Kyker-Snowman K, et al. Increased bone density in mice lacking the proton receptor OGR1. *Kidney Int*. 2016;89:565–573.
61. Yang M, Mailhot G, Birnbaum MJ, et al. Expression of and role for ovarian cancer G-protein-coupled receptor 1 (OGR1) during osteoclastogenesis. *J Biol Chem*. 2006;281:23598–23605.
62. Iwai K, Koike M, Ohshima S, et al. RGS18 acts as a negative regulator of osteoclastogenesis by modulating the acid-sensing OGR1/NFAT signaling pathway. *J Bone Miner Res*. 2007;22:1612–1620.
63. Li H, Wang D, Singh LS, et al. Abnormalities in osteoclastogenesis and decreased tumorigenesis in mice deficient for ovarian cancer G protein-coupled receptor 1. *PLoS ONE*. 2009;4:e5705.
64. Gong Y, Hou J. Claudins in barrier and transport function—the kidney. *Pflügers Arch*. 2017;469:105–113.
65. Muto S. Physiological roles of claudins in kidney tubule paracellular transport. *Am J Physiol Renal Physiol*. 2017;312:F9–F24.
66. Wei W-C, Jacobs B, Becker EBE, et al. Reciprocal regulation of two G protein-coupled receptors sensing extracellular concentrations of Ca2+ and H+. *Proc Natl Acad Sci U S A*. 2015;112:10738–10743.
67. Loon EPM van, Little R, Prehar S, et al. Calcium extrusion pump PMCA4: a new player in renal calcium handling? *PLoS One*. 2016;11:e0153483.
68. Lee C-T, Shang S, Lai L-W, et al. Effect of thiazide on renal gene expression of apical calcium channels and calbindins. *Am J Physiol Renal Physiol*. 2004;287:F1164–F1170.
69. Nijenhuis T, Vallon V, van der Kemp AWCM, et al. Enhanced passive Ca2+ reabsorption and reduced Mg2+ channel abundance explains thiazide-induced hypocalciuria and hypomagnesemia. *J Clin Invest*. 2005;115:1651–1658.
70. Lee C-T, Ng H-Y, Lee Y-T, et al. The role of calbindin-D28k on renal calcium and magnesium handling during treatment with loop and thiazide diuretics. *Am J Physiol Renal Physiol*. 2016;310:F230–F236.
71. Alexander RT, Dimke H. Effect of diuretics on renal tubular transport of calcium and magnesium. *Am J Physiol Renal Physiol*. 2017;312:F998–F1015.
72. Bonny O, Edwards A. Calcium reabsorption in the distal tubule: regulation by sodium, pH, and flow. *Am J Physiol Renal Physiol*. 2013;304:F585–F600.
73. Weinstein AM. A mathematical model of distal nephron acidification: diuretic effects. *Am J Physiol Renal Physiol*. 2008;295:F1353–F1364.
74. Tomura H, Wang J-Q, Komachi M, et al. Prostaglandin I2 production and cAMP accumulation in response to acidic extracellular pH through OGR1 in human aortic smooth muscle cells. *J Biol Chem*. 2005;280:34458–34464.
75. No YR, He P, Yoo BK, et al. Regulation of NHE3 by lysophosphatidic acid is mediated by phosphorylation of NHE3 by RSK2. *Am J Physiol Cell Physiol*. 2015;309:C14–C21.
76. Watts BA, George T, Good DW. Aldosterone inhibits apical NHE3 and HCO 3—absorption via a nongenomic ERK-dependent pathway in medullary thick ascending limb. *Am J Physiol Renal Physiol*. 2006;291:F1005–F1013.
77. He P, Klein J, Yun C. Activation of Na+/H+ exchanger NHE3 by angiotensin II is mediated by inositol 1,4,5-triphosphate (IP3) receptor-binding protein released with IP3 (IRBIT) and Ca2+/calmodulin-dependent protein kinase II. *J Biol Chem*. 2010;285:27869–27878.
78. Zachos NC, Hodson C, Kovbasnjuk O, et al. Elevated intracellular calcium stimulates NHE3 Activity by an IKEPP (NHERF4) dependent mechanism. *Cell Physiol Biochem*. 2008;22:693–704.
79. Wang Y, de Vallière C, Silva PHI, et al. The proton-activated receptor GPR4 modulates intestinal inflammation. *J Crohns Colitis*. 2018;12:355–368.
80. Russell JL, Goetsch SC, Aguilar HR, et al. Regulated expression of pH sensing G protein-coupled receptor-68 identified through chemical biology defines a new drug target for ischemic heart disease. *ACS Chem Biol*. 2012;7:1077–1083.
81. Huang X-P, Karpiak J, Kroeze WK, et al. Allosteric ligands for the pharmacologically dark receptors GPR68 and GPR65. *Nature*. 2015;527:477.